SLAC-PUB-2660
January 1981
T/E

INTRINSIC HEAVY QUARK STATES*

S. J. Brodsky and C. Peterson†

Stanford Linear Accelerator Center
Stanford University, Stanford, California 94305

N. Sakai‡

Fermi National Accelerator Laboratory
Batavia, Illinois 60510

ABSTRACT

The postulate that ordinary hadrons contain intrinsic charm quark states (such as $|uudc\bar{c}\rangle$ in the proton) at the 1% level is shown to explain two sets of unexpected experimental results: (1) the copious diffractive production of charmed hadrons at large longitudinal momentum in high energy proton-nucleon and pion-nucleon collisions, and (2) the anomalously large number of same-sign dimuon events observed in deep inelastic neutrino reactions. We also predict cross sections for open b- and t-production for high energy hadron-hadron collisions.

Submitted to Physical Review D

---

*Work supported in part by the Department of Energy under contract DE-AC03-76SF00515 and by the Swedish National Science Research Council under contract F-PD8207-101.

†On leave of absence from NORDITA, Copenhagen.

‡Present address: Department of Physics, Faculty of Science, Tohoku University, Sendai, 980 Japan.

I. INTRODUCTION

Although the nucleon is usually regarded as a three-quark bound state, its actual Fock state structure in quantum chromodynamics must be much more complicated. If we define the state at equal time on the light-cone (equivalent to the infinite momentum frame) then the proton has a general decomposition in terms of color-singlet eigenstates of the free Hamiltonian[1,2]

$$|uud\rangle\ , \qquad |uudg\rangle\ , \qquad |uudq\bar{q}\rangle\ , \ \ldots \tag{1}$$

Since hadrons are color singlets, all infrared divergences cancel and each of the amplitudes $\langle p|uud\rangle$, etc., have a well-defined probability.[2,3]

In this paper we shall explore the consequences of heavy quark pairs $Q\bar{Q}$ in the Fock state decomposition of the bound state wavefunction of ordinary mesons and baryons. Although proton states such as $|uudc\bar{c}\rangle$ and $|uudb\bar{b}\rangle$ are surely rare, the existence of hidden charm and and other heavy quarks within the proton bound state will lead to a number of striking phenomenological consequences.

It will be important to distinguish two types of contributions to the hadron quark and gluon distributions: extrinsic and intrinsic. Extrinsic quarks and gluons are generated on a short time scale in association with a large transverse momentum reaction; their distributions can be derived from QCD bremsstrahlung and pair production processes and lead to standard QCD evolution. The intrinsic quarks and gluons exist over a time scale independent of any probe momentum, and are associated with the bound state hadron dynamics. In particular, we expect the

presence of intrinsic heavy quarks $c\bar{c}$, $b\bar{b}$, etc., within the proton state by virtue of gluon exchange and vacuum polarization graphs as illustrated in Fig. 1, where all the colored particles are confined by the effective QCD potential. In fact, by using such a mechanism in the MIT bag model, Donoghue and Golowich[5] have estimated that the probability of finding a five-quark $|uudc\bar{c}\rangle$ configuration bound within the nucleon bag is at the order of 1 to 2%; i.e., the mean number $n_{c/p}$ of intrinsic charmed quarks within the proton is 0.01 to 0.02.

For heavier $Q\bar{Q}$ configurations the vacuum polarization mechanism of Fig. 1 evidently leads to the scaling

$$\frac{n_Q}{n_c} \sim \left(\frac{m_c}{m_Q}\right)^2 \frac{\alpha_s^2\left(m_Q^2\right)}{\alpha_s^2\left(m_c^2\right)} \quad , \tag{2}$$

i.e., $n_b/n_c \sim 0.1$ and $n_t/n_c \sim 0.005$ for $m_t = 20$ GeV.

The most striking property of an intrinsic heavy quark state such as $|uudQ\bar{Q}\rangle$ is that the heavy constituents tend to carry the largest fraction of the momentum of the hadron: $\langle x_Q \rangle > \langle x_q \rangle$. This general feature follows simply from the fact that the constituents in a moving bound state tend to have the same velocity; thus to first approximation the quark momentum $p_Q = E_Q v$ and $x_Q = \frac{p_Q + E_Q}{p + E}$ scale with its mass. In contrast, the perturbative production of extrinsic quark pairs occurs dominantly at wee $x \sim 0$; the extrinsic quark distribution falls even faster than the gluon distributions at large x.

The existence of the intrinsic charm component in the proton wavefunction then leads to the following consequences:

(1) The deep inelastic structure functions of nucleons (and other light hadrons) contain charm quarks at large x_{Bj}.

(2) Intrinsic charm states will be diffractively dissociated in high energy hadron collisions, producing open charm ($pN \to \Lambda_c X$, $pN \to DX$, etc.) in the large x_L beam and target fragmentation regions. The recent observation of such processes at the ISR and FNAL[6-13] gives a strong confirmation of this picture. We also predict that hidden charm states ψ, χ, η_c, etc., will also be diffractively produced in the fragmentation region, but at much lower rates compared to open charm. As we discuss in Sec. 9, the standard "fusion" subprocesses $gg \to \eta_c$, $q\bar{q} \to \psi$, etc., undoubtedly dominate hidden charm production in hadron collisions.

(3) Entirely new types of charged current reactions become possible using the intrinsic charm components of nucleons. For example, the reaction $\nu\bar{c} \to \mu^- \bar{b} \hookrightarrow \mu^- X$ illustrated in Fig. 2 yields a source of <u>same-sign</u> dimuon pairs $\nu N \to \mu^-\mu^- X$ (with the second μ^- in the current fragmentation region). Our predictions for these reactions are consistent with recent data (see Sec. 7). These events can occur on $\bar{c}$ quarks with large x_{Bj} and are accompanied by charm particles produced in the target fragmentation region.

The existence of intrinsic charm quarks in the proton wavefunction gives a new perspective on ordinary hadron structure. It must then also follow that instrinsic gluons, $u\bar{u}$ and $d\bar{d}$ sea quarks, and strange quarks exist in the hadron Fock state,[14] apart from distributions generated by QCD evolution. The assumption that the nucleon wavefunction can be regarded as a simple 3-quark amplitude at some fixed scale Q_0 thus becomes

untenable.

The most important phenomenological consequences of the intrinsic heavy quark components are the implications for beauty and truth hadron production in $p\bar{p}$ collisions at SPS and FNAL collider energies. If our prediction, Eq. (2), for heavy quark probabilities is correct then the diffractive cross sections for open beauty and truth at large energy ($\sqrt{s} \gtrsim 1$ TeV) will be surprisingly large

$$\sigma(p\bar{p} \to Q\bar{Q}X) \sim \frac{m_c^2}{m_Q^2}\, \sigma(p\bar{p} \to c\bar{c}X) \tag{3}$$

$$\sim \begin{cases} 70\ \mu b\ \text{(beauty) with } m_b = 5\ \text{GeV} \\ 3\ \mu b\ \text{(truth) with } m_t = 20\ \text{GeV} \end{cases}$$

using an extrapolated value 700 μb for $\sigma(p\bar{p} \to c\bar{c}X)$ (see Sec. V). Furthermore, since the intrinsic transverse momentum associated with the $|uudQ\bar{Q}\rangle$ states tends to increase monotonically with the quark mass (see Sec. III) the Q and $\bar{Q}$ hadron jets are expected to be produced at relatively large transverse momentum.

This paper is organized as follows: in Sec. II we briefly review the experimental results on charm production and discuss how conventional models fail to explain the data. Section III contains a general discussion on non-perturbative properties of hadronic wavefunctions, and model distributions for $|qqqQ\bar{Q}\rangle$ and $|q\bar{q}Q\bar{Q}\rangle$ states are derived. In Sec. IV we calculate inclusive hadron spectra for open charm production and the energy dependence is discussed in Sec. V. Section VI contains predictions for top and beauty cross sections at ISR and Tevatron energies. Conse-

quences of the intrinsic charm pictures for neutrino production of same-sign dimuons and "wrong-sign" muons are derived in Sec. VII and VIII, respectively. Several important factors of ψ-suppression relative to open charm productions are given in Sec. IX and finally Sec. X contains the conclusions.

II. CHARM PRODUCTION AT HIGH ENERGIES

One of the most important results obtained at the ISR has been the observation of charm production in pp collisions with remarkably large cross sections and quite unexpected momentum distributions:[6-12]

(1) The cross sections observed for $pp \to \Lambda_c^+ X$ and $pp \to D^+ X$ at $\sqrt{s}$ = 53 and 63 GeV are of the order of 0.1 to 0.5 mb.

(2) The charmed hadrons are produced abundantly in the forward regions of phase space (see Figs. 3-5), contrary to standard expectations. In particular, the D^+, which shares no valence quarks with the proton, would have been expected to be suppressed in the proton fragmentation region. In fact, its Feynman-x distribution seems to be roughly flat in the measured region ($0 \leq x_F \leq 0.4$) and relatively flat in p_T. Moreover, at least one experiment,[7] which triggers a single proton in the other CM hemisphere, strongly suggests a diffractive dissociation mechanism for the production.[13] More recently, the Illinois-Fermilab-Harvard-Oxford-Tufts collaboration at Fermilab[12] has observed the reaction $\pi^- p \to D\bar{D}pX$ at E_{lab} = 217 GeV ($\sqrt{s}$ = 20.2 GeV) with a slow recoil proton trigger. The diffractive $\pi^- p \to D\bar{D}pX$ cross sections are of order 10 μb. The charged $D^{\pm}$ production again shows abundant production of charm at large

x_F, peaking at $x_F \sim 0.4$ (see Fig. 5).

It is difficult to understand the physics of these charm production cross sections from the standpoint of conventional dynamical mechanisms.[15] Although it is expected that perturbative QCD should be applicable to heavy quark production, the predicted QCD cross sections are of order 10-50 μb at ISR energies[22] and fall steeply with x_F, certainly faster than the gluon distributions. In triple-Regge models, charm production at large x_F is strongly suppressed by the low intercept of the charmed particle trajectories. In models based on conventional soft hadronization mechanisms, charm pair production is strongly suppressed by factors like $\exp[-\pi\alpha'_R M_Q^2]$. Most important, it is impossible to explain the observed forward produced D^+ in pp collisions from any valence quark recombination or quark fragmentation model, since none of the proton valence quarks are contained in a D^+.

It is evident from the accumulating data that a new dynamical mechanism is involved in open charm production. Since the experiments indicate that a short time scale perturbative picture of charm production is not adequate, we shall explore the consequences of the existence of "intrinsic" (long time-scale) charm components in the proton bound state.[16] As discussed in the introduction, we assume that the number of charmed quarks per nucleon is at the 1 to 2% level.

It is clear that intrinsic charm states are easily dissociated into open charm hadrons at high energy collisions (see Fig. 6). The production can be diffractive at high energies since only small momentum transfers are needed. In fact, a 300 μb charm production cross section can be easily understood if ~ 1% of all pp inelastic events involve dissociation

of the intrinsic charm state.

Since the mass of the diffractively excited state M should be much larger than the heavy quark mass one does not expect cross sections at this magnitude until high energies. A detailed discussion of the energy dependence is given in Sec. V.

III. HADRONIC WAVE FUNCTIONS

As we have discussed in the introduction, the hadronic wavefunction in QCD has a well-defined Fock state decomposition at equal time on the light cone in terms of quark and gluon momentum states.[4] The wavefunction amplitude for each Fock component has the form

$$\psi_{(n)}(\vec{k}_{\perp i}, x_i) \quad , \quad 0 \le x_i \le 1 \quad , \quad i = 1,\ldots,n \tag{4}$$

where by momentum conservation $\sum_{i=1}^{n} x_i = 1$ and $\sum_{i=1}^{n} k_{\perp i} = 0$. The x_i are the light-cone (infinite momentum frame) momentum fractions $(k^0 + k^3)/(p^0 + p^3)$ for each constituent. (Spin labels are suppressed.) The state is off the $p^- = p^0 - p^3$ mass shell

$$p^- - \sum_{i=1}^{n} k^- = \frac{1}{p^+}\left(M^2 - \sum_{i=1}^{n}\left(\frac{k_\perp^2 + m^2}{x}\right)_i\right) \quad . \tag{5}$$

The standard quark and gluon distributions are obtained from integrating the square of the wavefunctions up to the momentum scale Q of the probe and summing over all Fock states

$$G_{q/p}(x,Q^2) \propto \sum_n \int^{Q} [d^2k_\perp][dx]\, \delta(x-x_q) \left|\psi_{(n)}(k_{\perp i}, x_i)\right|^2 \quad . \tag{6}$$

The "extrinsic" quarks and gluons correspond to the standard bremsstrahlung and $q\bar{q}$ pair production processes of perturbative QCD. These perturbative contributions yield wavefunctions with minimal power-law fall-off

$$|\psi(k_{\perp i}, x_i)|^2 \sim \frac{1}{k_{\perp i}^2} \tag{7}$$

and lead to the logarithmic evolution of the structure functions. In contrast, the intrinsic contributions to the quark distribution are associated with the bound state dynamics and necessarily have a faster fall-off in $k_{\perp i}$ ($\psi \sim 1/k_\perp^2$ or faster[2]). The intrinsic states thus contribute to the initial quark and gluon distributions. A simple illustration of extrinsic and intrinsic $|uudq\bar{q}\rangle$ contributions to the deep inelastic structure functions is shown in Fig. 7a and b. We see that existence of gluon exchange graphs, plus vacuum polarization insertions, automatically yield an intrinsic $|uudq\bar{q}\rangle$ Fock state.[14] Even if we imagined that in the nucleon rest frame there are effectively only 3 quarks in the nucleon, the gluon exchange diagrams automatically generate $|uudg\rangle$ and $|uudq\bar{q}\rangle$ components when boosted to infinite momentum or the light cone. In fact, the magnitude of the $P - \Delta$ hyperfine splitting due to transversely polarized gluon exchange must yield a lower bound on the intrinsic gluon and $q\bar{q}$ components.[17] A complete calculation must take into account the binding of the gluon and $q\bar{q}$ constituents inside the hadron (see Fig. 1) so that the analysis is necessarily non-perturbative.

We also note that the normalization of the $|uudq\bar{q}\rangle$ state is not necessarily tied to the normalization of the $|uudg\rangle$ components since the

latter only refers to transversely polarized gluons. Figure 1b shows that $q\bar{q}$ pairs also arise from the longitudinal-scalar (instantaneous) parts of the vector potential.

The general form of a Fock state wavefunction is

$$\psi(k_{\perp i}, x_i) = \frac{\Gamma(k_{\perp i}, x_i)}{M^2 - \sum_{i=1}^{n} \left(\frac{m^2 + k_\perp^2}{x}\right)_i} \tag{8a}$$

where Γ is the truncated wavefunction or vertex function. The actual form of Γ must be obtained from the non-perturbative theory, but following Ref. 4 it is reasonable to take Γ as a decreasing function of the off-energy-shell variable $\mathscr{E} = M^2 - \sum_{i=1}^{n} \left(\frac{m^2 + k_\perp^2}{x}\right)_i$. Independent of the form $\Gamma(\mathscr{E})$, we can read off some general features of the quark distributions:

(1) In the limit of zero binding energy ψ becomes singular and the fractional momentum distributions peak at the values $x_i = m_i/M$. More generally, $\mathscr{E}$ is minimal and the longitudinal momentum distributions are maximal when the constituents with the largest transverse mass $m_\perp = \sqrt{m^2 + k_\perp^2}$ have the largest light-cone fraction x_i. This is equivalent to the statement that constituents in a moving bound state tend to have the same rapidity.

(2) The intrinsic transverse momentum of each quark in a Fock state generally increases with the quark mass. In the case of power law wavefunction $\psi \sim (\mathscr{E})^{-\beta}$ we have $\langle k_\perp^2 \rangle \propto \langle m_Q^2 \rangle$; for an exponential wavefunction $\psi \sim e^{-\beta \mathscr{E}^{1/2}}$, the dependence is $\langle k_\perp^2 \rangle \propto m_Q$.

In the limit of large $k_\perp$ one can use the operator product expansion

near the light cone (or equivalently gluon exchange diagrams) to prove that, modulo logarithms, the Fock state wavefunctions fall off as inverse powers of $k_\perp^2$.[2] For our purpose, which is to illustrate the characteristic shape of the Fock states containing heavy quarks, we will choose a simple power-law form for the Fock state longitudinal momentum distributions

$$P_{(n)}(x_1 \ldots\ldots x_n) = N_{(n)} \frac{\delta\left(1 - \sum_{i=1}^{n} x_i\right)}{\left(M^2 - \sum_{i=1}^{n} \frac{\hat{m}_i^2}{x_i}\right)^2} \tag{8b}$$

where the $\hat{m}_i^2$ are identified now as effective transverse masses $\hat{m}_i^2 = m_i^2 + \langle k_\perp^2 \rangle_i$ and the $\langle k_\perp^2 \rangle$ are average transverse momentum. With this choice, single-quark distributions have power-law fall-offs $(1-x)^2$ and $(1-x)^3$ for mesons and baryons, respectively.

For example, consider a $|\bar{q}Q\rangle$ state, e.g., a D-meson. Here the momentum distributions of the 2 quarks are according to Eq. (8b) given by

$$P(x_1,x_2) = N \frac{\delta(1 - x_1 - x_2)}{\left(m_D^2 - \frac{\hat{m}_c^2}{x_1} - \frac{\hat{m}_u^2}{x_2}\right)^2} \quad . \tag{9}$$

From this expression we obtain the charmed quark distribution

$$P(x_1) = \int_0^{1-x_1} P(x_1,x_2)dx_2 = N' \frac{1}{\left(1 - \frac{1}{x_1} - \frac{\varepsilon}{1-x_1}\right)^2} \tag{10}$$

where $N' = \frac{N}{m_D^4}$, $\varepsilon = \frac{\hat{m}_u^2}{m_D^2}$ and we take $m_D^2 \approx \hat{m}_c^2$. We see from Fig. 8 that

the c-quark tends to carry most of the D-meson momentum ($\langle x_1 \rangle = 0.73$). This leading feature of the c-quark is due to the fact that the quarks should have roughly the same velocity in order for the hadron to "stay together". This can be seen more explicitly by minimizing the off-shellness, i.e., the denominator in Eq. (9)

$$\frac{\hat{m}_c^2}{x_1^2} = \frac{\hat{m}_u^2}{x_2^2} \tag{11}$$

keeping the transverse masses fixed. (A related idea has previously been considered by Bjorken and Suzuki[18] in the context of charm fragmentation into hadrons.)

We now turn to the discussion of $|uudQ\bar{Q}\rangle$ and $|u\bar{d}Q\bar{Q}\rangle$ states. For a $|uudc\bar{c}\rangle$ proton Fock state the momentum distribution is given by

$$P(x_1,\ldots,x_5) = N \frac{\delta\left(1 - \sum_{i=1}^{5} x_i\right)}{\left(m_p^2 - \sum_{i=1}^{5} \frac{\hat{m}_i^2}{x_i}\right)^2} \quad . \tag{12}$$

In the limit of heavy quarks $\hat{m}_4^2 = \hat{m}_5^2 >> m_p^2$, $\hat{m}_i^2$ $(i = 1,2,3)$ we get

$$P(x_1,\ldots,x_5) = N_5 \frac{x_4^2 x_5^2}{(x_4 + x_5)^2} \delta\left(1 - \sum_{i=1}^{5} x_i\right) \tag{13}$$

where $N_5 = 3600\ P_5$ is determined from $\int dx_1 \ldots dx_5 P(x_1,\ldots,x_5) = P_5$, where P_5 is the $|uudc\bar{c}\rangle$ Fock state probability. Integrating over the light quarks (x_1, x_2 and x_3) we get the charmed quark distributions

$$P(x_4,x_5) = \frac{1}{2} N_5 \frac{x_4^2 x_5^2}{(x_4 + x_5)^2} (1 - x_4 - x_5)^2 \quad . \tag{14}$$

By performing one more integration we obtain the charmed quark distribution

$$P(x_5) = \frac{1}{2} N_5 x_5^2 \left[\frac{1}{3}(1 - x_5)(1 + 10x_5 + x_5^2) - 2x_5(1 - x_5)\log \frac{1}{x_5}\right] \tag{15}$$

which has average $\langle x_5 \rangle = 2/7$ and is shown in Fig. 9. This is to be contrasted with the corresponding light quark distribution derived from Eq. (13) and shown in Fig. 10

$$P(x_1) = 6(1 - x_1)^5 P_5 \quad . \tag{16}$$

We estimate P_5 from the magnitude of "diffractive" production of Λ_c(pp → pΛ_cX)[6]

$$P_5 = P(|uudc\bar{c}\rangle) = \frac{\sigma_{\Lambda_c}}{\sigma_{tot}} \simeq \frac{300\ \mu b}{40\ mb} \approx 0.01 \tag{17}$$

in agreement with the bag model estimate.[5] The charmed quark distribution $c(x) = P(x_5)$ should be measurable in lepto-production for high enough Q^2 and $W^2 > W_{th}^2 = 25\ GeV^2$. Hence to measure c(x) at, e.g., x = 0.5 requires $Q^2 = 37.5\ GeV^5$ ($x = Q^2/(Q^2+W^2)$). In Fig. 11 we show the same quantity, both c(x) from the intrinsic sea and the one calculated from perturbative QCD[19] at $Q^2 = 50\ GeV^2$. We have neglected the small Q^2 evolution of the intrinsic charmed sea.

From Fig. 11 we see that intrinsic charmed quarks in the proton are

"rare" but not "wee". Needless to say, high x_{Bj} lepto-production data would provide a most crucial test of the intrinsic idea. At present, data only exist for small $x < 0.13$ and seem to be adequately described by the photon-gluon fusion model.[20] Note that the intrinsic charm component gives single charm quark jets in the current fragmentation region, whereas the photon-gluon fusion model[21] gives two jets (charm and anticharm), (see Fig. 12).

We next compute the corresponding x-distributions for meson Fock states, e.g., $|u\bar{d}c\bar{c}\rangle$. Again neglecting meson and light quark masses compared to the heavy quark mass, we get

$$P(x_1,\ldots,x_4) = N_4\left(\frac{x_3x_4}{x_3 + x_4}\right)^2 \delta\left(1 - \sum_{i=1}^{4} x_i\right) \tag{18}$$

where $x_3 = x_c$, $x_4 = x_{\bar{c}}$ and $N_4 = 600\ P_4$. By integrating over x_1, x_2, x_3 we obtain the single quark distribution

$$P(x_4) = N_4 x_4^2\left[\frac{1}{2}(1 + 4x_4 - 5x_4^2) + x_4(2 + x_4)\log x_4\right] \tag{19}$$

which is shown in Fig. 13 and has $\langle x_4\rangle = 1/3$. The corresponding light quark spectrum from Eq. (18) is given by

$$P(x_1) = 5(1 - x_1)^4\ P_4 \tag{20}$$

with $\langle x_1\rangle = 1/6$ is shown in Fig. 14.

It should be remarked that the $\hat{m}_Q \to \infty$ approximations used above are quite accurate. It turns out that keeping the masses implies that the denominator $(x_3 + x_4)$ in Eq. (13) above is just replaced by

$(x_3 + x_4 + \varepsilon x_3 x_4)$ where $\varepsilon = \frac{m_p^2}{\hat{m}_Q^2}$ leading to only a few percent corrections. The light quark distributions (Eqs. (16) and (20)) will be hidden in the perturbative extrinsic sea of the hadron in large momentum transfer experiments.

IV. INCLUSIVE CHARM PRODUCTION AND HADRON-HADRON COLLISIONS

As was discussed in Sec. II it is reasonable to assume that the intrinsic heavy quark states, $|qqqc\bar{c}\rangle$ and $|q\bar{q}c\bar{c}\rangle$, should be "fragile" and can be materialized into open charm hadrons in high energy, low momentum transfer reactions. In principle, the Λ_c and D spectra can be calculated from the strong overlap between the 5-quark and the charmed-hadron state wavefunctions, allowing for decays of excited state, etc. For the purpose of obtaining the x_F-distributions we shall use a simple recombination mechanism for the quarks involved in the states. Neglecting its binding energy, the Λ_c spectrum is given by combining the u, d and c-quark in $|uudc\bar{c}\rangle$ to obtain

$$P(x_{\Lambda_c}) = N_5 \int_0^1 \prod_{i=1}^{5} dx_i \delta(x_{\Lambda_c} - x_2 - x_3 - x_4) \left(\frac{x_4 x_5}{x_4 + x_5}\right)^2 \delta\left(1 - \sum_{i=1}^{5} x_i\right) \qquad (21)$$

(see Fig. 15) with $\langle x_{\Lambda_c} \rangle = \frac{1}{7} + \frac{1}{7} + \frac{2}{7} = \frac{4}{7}$. The ISR data for $\frac{d\sigma}{dx}(pp \to \Lambda_c X)$ (see Fig. 3a) are consistent with the prediction of Eq. (2I) that charmed baryons are produced in the forward fragmentation region, although the existing data are too scarce for a detailed comparison. We expect that the low x region for charm production will be filled in by both perturbative and higher Fock state intrinsic contributions. The corresponding distribution for $D^-(\bar{c}d)$ is given by

$$P(x_{D^-}) = N_5 \int_0^1 \prod_{i=1}^{5} dx_i \delta(x_{D^-} - x_3 - x_5) \left(\frac{x_4 x_5}{x_4 + x_5}\right)^2 \delta\left(1 - \sum_{i=1}^{5} x_i\right) \qquad (22)$$

with $\langle x_{D^-} \rangle = \frac{1}{7} + \frac{2}{7} = \frac{3}{7}$, and is shown in Fig. 16. The $D^+(c\bar{d})$ distribution would, in principle, be obtained from the $|uudc\bar{c}d\bar{d}\rangle$ Fock state of the proton, where the $d\bar{d}$ could be extrinsic or intrinsic. Assuming that the $\bar{d}$ momentum is small, the D^+ distribution should be close to that of the c-quark shown in Fig. 12. These predictions apply for forward production ($x_F \gtrsim 0.1$), where perturbative contributions and higher Fock state contributions can be neglected.

For the π-fragmentation region in the reaction $\pi p \to D\bar{D}X$ the x_F-distribution of the D's is obtained in the same way:

$$P(x_D) = N_4 \int \prod_{i=1}^{4} dx_i \delta(x_D - x_1 - x_3) \left(\frac{x_3 x_4}{x_3 + x_4}\right)^2 \delta\left(1 - \sum_{i=1}^{4} x_4\right) \qquad (23)$$

with $\langle x_D \rangle = \frac{1}{2}$. $P(x_D)$ is shown in Fig. 17 and again we observe that the intrinsic model gives a consistent picture of the forward nature of the charm production data. (Compare Fig. 5.)

V. ENERGY DEPENDENCE OF HADROPRODUCTION OF HEAVY QUARKS

For perturbative heavy quark production mechanisms such as the gluon-gluon fusion model[22] the energy dependence of the cross section essentially comes from the lower limit $m_Q/(2\sqrt{s})$ of convolution integrals, and gives rise to a logarithmic energy dependence. To study the energy dependence of the "diffraction" mechanism with "intrinsic" heavy quarks we will use the empirical formula for high mass diffraction[23]

$$\frac{d\sigma}{dM^2} = \sigma_0 \frac{1}{M^2} \tag{24}$$

valid for $M^2 \gtrsim 2$ GeV^2. The integrated charm cross section is given by

$$\sigma = \sigma_0^c \int_{M_0^2}^{M_1^2} \frac{dM^2}{M^2} = \sigma_0^c \log \frac{(1 - x_1)s}{\left(M_{\Lambda_c} + M_D\right)^2} \quad , \tag{25}$$

where in this case M_0^2 is the threshold value for associated production of a pair of hadrons containing charmed quarks. The upper limit M_1^2 is determined from the kinematical relation $M_1^2 = s(1 - x_1)$ where x_1 is the lower fractional momentum cut on the recoiling proton. In the ISR $pp \to p_1 \Lambda_c X$ experiment[7] one triggers on events with $x_1 \geq 0.8$. If we assume that essentially all the charm cross section $\sigma_c \sim 300$ μb is due to diffractive production, then we can determine $\sigma_0 = 77$ μb. We thus predict that at SPS and FNAL energies ($s \cong 400$-600 GeV^2), the total $pp \to$ charm cross section should be of the order of 150 μb. The beam dump experiment (model dependent),[24] which can be interpreted in terms of charm production gives cross sections of up to 80 ± 40 μb. The pion-induced diffractive charm cross section at FNAL at $s = 416$ GeV^2 is ~ 10 μb. This could imply that the probability for intrinsic charm is smaller for the pion than the proton.

We also note that concerning production of heavy quarks on nuclear targets one expects a $A^{2/3}$-dependence from the intrinsic charm model. This is in contrast to the perturbative hard scattering cross section, which should be proportional to A.

VI. PRODUCTION OF b- AND t-QUARKS

We now estimate the associated production of beauty and truth hadrons from the intrinsic sea from Eq. (24). As discussed in the introduction,

we expect a $\sim 1/m_Q^2$ dependence for the suppression of intrinsic heavy quarks. The prediction for the diffractive beauty cross section at the ISR ($\sqrt{s}$ = 63 GeV^2) is

$$\sigma^b = \left(\frac{m_c}{m_b}\right)^2 \sigma_0^c \int_{(2m_b)^2}^{0.2s} \frac{dM^2}{M^2} \approx 15 \quad \mu b \tag{26}$$

using the value for σ_0^c determined from charm production. The Λ_b spectrum should have the same shape as the Λ_c. This cross section should be compared with those predicted from perturbative mechanisms[22] for the central region: $\sigma^b \cong 0.1$ μb. If $m_t \gtrsim 20$ GeV, then t-quark hadron production is kinematically suppressed at ISR energies. At Tevatron collider energies ($\sqrt{s} = 2.10^3$ GeV) we expect for b-production with $M_1^2 = 0.25s$

$$\sigma^b = 73 \ \mu b$$

and for t-production (assuming $m_t = 20$ GeV)

$$\sigma^t = \left(\frac{m_c}{m_t}\right)^2 \sigma_0^c \int_{(2m_t)^2}^{0.2s} \frac{dM^2}{M^2} \approx 3 \quad \mu b \quad . \tag{27}$$

The corresponding values from hard mechanisms[22] at these energies are

$$\sigma^b \approx 2 \ \mu b \qquad \text{and} \qquad \sigma^t \approx 0.1 \ \mu b.$$

Not only are the intrinsic cross sections larger than perturbative contributions, but also the combinatorial background is reduced in diffractive configurations. In addition, since the transverse momentum of heavy quarks in the intrinsic state generally increases with the quark mass

(see Sec. II), the heavy quark hadrons are produced at relatively large transverse momentum.

VII. SAME-SIGN DIMUON PRODUCTION

The presence of intrinsic charm in the proton at the 1 and 2% level makes possible a number of new charged and neutral weak current interactions. We will consider neutral current phenomena in Chap. VIII. Perhaps the most interesting implication of intrinsic charm for νN and $\bar{\nu}N$ charge current reactions is the production of beauty quarks ($\bar{\nu}c \to \mu^+ b$ and $\nu\bar{c} \to \mu^- b$). The subsequent leptonic decay of the b and $\bar{b}$ then leads to same-sign muon pairs (see Fig. 2). We will also briefly discuss t-production via $b \to t$ charged currents.

In principle, charged current b-production can proceed via the process $\bar{\nu}u \to \mu^+ b$, $\bar{\nu}c \to \mu^+ b$ and $\bar{\nu}t \to \mu^+ b$. The t-quark intrinsic sea is negligible in this connection ($P(uud t\bar{t}) \sim (m_c^2/m_t^2)\, P(uudc\bar{c})$; see Eq. (2)). For the first two reactions we need the u-b and c-b couplings. From a recent analysis[25] of the K-M matrix elements[39] we learn that the $u \to b$ coupling is small (0.004 ± 0.004). For the $c \to b$ charged current coupling there exist two solutions: $V_{cb} \cong 0.48\ G_F$ and $0.22\ G_F$, where G_F is the standard weak coupling constant. The differential cross section for $\bar{\nu}p \to \mu^+ b$ (see Fig. 18a) or $\nu p \to \mu^- b$ is given by

$$\frac{d\sigma}{dxdy} = \frac{m_N E_\nu x}{4\pi} (2\sqrt{2}G_F)^2 |V_{cb}|^2 c(x)(1-y)^2 \quad . \tag{28}$$

The integrated cross section $\sigma_{c \to b}(E_\nu)$ as a function of beam energy is obtained by using the kinetical restriction $2m_N\nu - Q^2 \geq 2m_N m_b + m_b^2$.[26]

In Fig. 19 we show $\sigma_{c \to b}(E_\nu)$ for the two V_{cb}-solutions. The subsequent decay of the produced b-quark as in $b \to c \to s\mu^+\nu$ gives rise to same-sign muons (see Fig. 18b). The resulting same-sign muon production cross section is given by $\sigma_{c \to b}(E_\nu)B(c \to \mu)$ where the branching ratio $B(c \to \mu)$ is $\simeq 0.15$.[27] In Fig. 18 the ratio $\mu^\pm\mu^\pm/\mu$ is plotted for isoscalar targets and compared with the experimental results. In fact, the measured[20] ratio $(\mu^\pm\mu^\pm)/\mu^+\mu^-)$ is as large as 0.1, an order of magnitude larger than what is predicted from first-order perturbative QCD associated charm production[29] (see Fig. 18). Intrinsic charm, however, is seen to give a good explanation of the large same-sign dimuon rate. In addition, in the BEBC experiment[30] a correlation of p_{μ^+} and total hadronic energy is observed; this could perhaps be interpreted as the production of a bottom baryon. It should be remarked, however, that the approximate agreement in Fig. 20 for same-sign dimuons is not very sensitive to the x_{Bj} distribution of the intrinsic charm sea, but only depends on its magnitude. Further experiments which can discriminate the x-distribution of c(x) are necessary. The $b(\bar{b})$ quark production in the charged current fragmentation region should be accompanied by associated charm $\bar{c}(c)$ production in the target fragmentation region.

Finally we consider the production of t-quarks through the $b \to t$ mechanism of Fig. 21. In Fig. 18 the result for $\sigma_{b \to t}(E)$ is displayed assuming the mass suppression m_b^{-2}.

The occurrence of intrinsic states such as $|uuds\bar{s}\rangle$ and $|uudc\bar{c}\rangle$ in the proton also allows the possibility of producing rather exotic baryons in exclusive charged-current reactions. Two examples are shown in Fig.

22, in which strange/charmed baryons and charm/beauty baryons are produced. The process illustrated in Fig. 22b would not be expected for the standard perturbative sea since the formation of the final baryon requires b-quarks with large x.

VIII. WRONG-SIGN MUON PRODUCTION

The intrinsic charm component in the proton can give abundant "wrong sing" single muon $\nu(\bar{\nu})$ reactions, $\nu N \to \mu^+ X$ and $\bar{\nu} N \to \mu^- X$. There is a rather stringent experimental bound on this ratio from the CDHS experiment[30]

$$R_{expt} = \frac{\sigma(\nu N \to \mu^+ X)}{\sigma(\nu N \to \mu^- X)} < 1.6 \times 10^{-4} \quad . \tag{29}$$

We will show that the intrinsic charm model gives a cross section consistent with this bound after taking into account an estimate of the experimental cuts.

Intrinsic charm contributes to the reaction $\nu N \to \mu^+ X$ through the neutral current interaction depicted in Fig. 23. The cross section for $\nu N \to \nu c X$ is given by[32]

$$\frac{d\sigma}{dxdy} = \frac{m_N E_\nu x}{4\pi} (2\sqrt{2} G_F)^2 \left[\left(\frac{1}{2} - \frac{2}{3} \sin^2\theta_W \right)^2 + \left(\frac{2}{3} \sin^2\theta_W \right)^2 (1-y)^2 \right] c(x). \tag{30}$$

If there were no experimental bias, we could obtain its ratio to the normal charged-current cross section in Eq. (30) by simply integrating over y

$$\left.\frac{\frac{d\sigma}{dx}(\nu N \to \nu c X)}{\frac{d\sigma}{dx}(\nu N \to \mu^- X)}\right|_{\text{uncorrected}} \simeq 0.135\,\frac{c(x)}{d(x)} \qquad (31)$$

where we used $\sin^2\theta_W \simeq 0.229$.[33]

An important constraint of the CDHS experiment comes from the cut in the total visible energy: $E_{vis} \equiv E_{hadron} + E_{\mu^+} > E_{cut}$. The probability for the neutral current event to survive the experimental cut is less than

$$\int_{y_c}^{1} dy\,\frac{d\sigma}{dxdy} \Big/ \int_{0}^{1} dy\,\frac{d\sigma}{dxdy} < 1 - y_c \qquad (32)$$

where $y_c \equiv E_{cut}/E_\nu$. (We have overestimated this probability by neglecting the energy carried by the neutrino from the decay of the c-quark.) The narrow band beam of the experiment has an approximately flat energy spectrum[34] extending up to E_0. Therefore, the correction factor due to the cut is on the average

$$\langle 1 - y_c \rangle = 1 - \frac{E_{cut}}{E_0 - E_{cut}}\,\ell n\,\frac{E_0}{E_{cut}} \qquad (33)$$

$$\simeq 0.29$$

where we used $E_0 \simeq 190$ GeV, $E_{cut} \simeq 100$ GeV. If we combine the factors (31), (32) and (33) with our estimate $\langle c(x)/d(x) \rangle \simeq 10^{-2}$ and the branching ratio $B(c \to \mu^+ X) \cong 0.15$, we obtain

$$R_{expt} = \frac{\sigma(\nu N \to \nu \mu^+ X)}{\sigma(\nu N \to \mu^- X)} \simeq 0.135\,\frac{c(x)}{d(x)}\,0.15 \times 0.29 \simeq 5.8 \times 10^{-5} \qquad (34)$$

consistent with the experimental bound, Eq. (29).[35]

IX. HADRONIC J/ψ PRODUCTION

In addition to charmed mesons and baryons, the J/ψ may also be produced diffractively from the intrinsic charm component of the proton. Compared to the charm production cross section at FNAL energies[11]

$$\sigma(\pi N \to DX) \simeq 20\ \mu b \quad , \tag{35}$$

J/ψ production data around 200 GeV give[36]

$$\sigma(\pi N \to \psi X) \simeq 100\ nb \quad .$$

Further, the observed x_F-distribution appears to be more strongly peaked near $x \simeq 0$ compared to what would be expected from the intrinsic charm distribution. Evidently most of the ψ production comes from other central production mechanisms such as gluon and $q\bar{q}$ fusion.[40] In order for the intrinsic charm model to be consistent, there must be a large suppression factor for the ψ production from the intrinsic charm compared to the D production

$$\left.\frac{\sigma(\pi N \to \psi X)}{\sigma(\pi N \to DX)}\right|_{\text{intrinsic charm}} \lesssim 5 \times 10^{-5} \quad . \tag{36}$$

Our general picture is as follows: after the incoming proton is diffractively dissociated, the $|uudc\bar{c}\rangle$ system can form either open or hidden charm states with roughly the same energy dependence. The probability of ψ production then depends on color and flavor combinatorics

and the "semi-local duality" probability of forming the color singlet state in the right mass range. In fact, there are a number of factors which act to suppress forward ψ production compared to open charm.

(1) In the decay of the $|uudc\bar{c}\rangle$ state, the probability that the $\bar{c}$ quark combines to form a $c\bar{c}$ system is about 1/4 (flavor suppression). Similarly, the flavor suppression factor for the $|u\bar{d}c\bar{c}\rangle$ state is about 1/2.

(2) A $c\bar{c}$ system can be formed in either a color octet $c\bar{c}$ or singlet $c\bar{c}$ state. The color octet $c\bar{c}$ state should interact with other colored particles and is most likely to decay into open charm particles such as D's. Therefore, we can take only the color singlet combination of $c\bar{c}$ for ψ production. This occurs only 1/9 of the time (color suppression).

(3) If the color singlet $c\bar{c}$ system has a mass larger than the $D\bar{D}$ threshold, it will decay strongly into charmed particles rather than ψ production. Therefore, we have to require that the invariant mass $M_{c\bar{c}}$ is below the $D\bar{D}$ threshold (mass suppression)

$$2m_c < M_{c\bar{c}} < 2m_D \quad . \tag{37}$$

If we neglect transverse momenta, the simplified model of the intrinsic charm state $|uudc\bar{c}\rangle$ gives a mass spectrum [see Eq. (14)]

$$\frac{dP}{dM^2_{c\bar{c}}} = \frac{N}{m_c^2}\left(\frac{m_c^2}{M^2_{c\bar{c}}}\right)^4 \int_{\frac{4m_c^2}{M^2_{c\bar{c}}}}^{1} dx(1-x)^2 \frac{\sqrt{x}}{\sqrt{x - \frac{4m_c^2}{M^2_{c\bar{c}}}}} \tag{38}$$

$$M^2_{c\bar{c}} = \frac{m_c^2}{x_c} + \frac{m_c^2}{x_{\bar{c}}}$$

$$x = x_c + x_{\bar{c}}$$

$$N = 3600$$

which is shown in Fig. 24. The approximate mass spectrum near threshold is given by

$$\frac{dP}{dM^2_{c\bar{c}}} \simeq \frac{15}{32} \frac{\left(M^2_{c\bar{c}} - 4m_c^2\right)^{5/2}}{m_c^7} \quad . \tag{39}$$

In addition, the transverse momenta of c-quarks suppress the mass spectrum near threshold even more strongly. We shall simulate this effect by effectively increasing m_c ($m_c^2 \to \hat{m}_c^2 = m_c^2 + \langle k_1^2 \rangle$).[37] If we take $\hat{m}_c \simeq 1.7$ GeV for instance, we obtain

$$\int_{4\hat{m}_c^2}^{4m_D^2} dM^2_{c\bar{c}} \frac{dP}{dM^2_{c\bar{c}}} \simeq 10^{-2} \quad . \tag{40}$$

(4) Even if the $c\bar{c}$ system is below $D\bar{D}$ threshold, it may be realized as χ, η_c and ψ' states which do not decay into ψ's. We estimate this suppression factor as 1/3 (channel suppression). If we combine the factors in (1)-(4) we obtain the very rough theoretical estimate

$$\left.\frac{\sigma(\pi N \to \psi X)}{\sigma(\pi N \to DX)}\right|_{\text{intrinsic charm}} \simeq 5 \times 10^{-5} \quad . \tag{41}$$

Despite these uncertainties, it is clear that although the intrinsic charm model does predict ψ production in the forward fragmentation region, the rate is at a very suppressed level.

X. CONCLUSION

The postulate that ordinary hadrons contain intrinsic charm states[16] at the 1% level can explain two sets of unexpected experimental results: (1) the copious diffractive production of charmed hadrons at large longitudinal momentum in high energy proton-nucleon and pion-nucleon collisions, and (2) the anomalously large number of same-sign dimuon events observed in deep inelastic neutrino reactions. Clearly, much more experimental work is necessary to verify and test the model and its predictions. Most important, it will be crucial to verify that the charm quark distribution $c(x)$ in nucleons is appreciable at large x_{Bj} in deep inelastic lepton scattering.

The concept that the wavefunction of an ordinary hadron has finite mixing with virtual bound states containing heavy quark pairs is a new dynamical concept and is somewhat at variance with standard parton model ideas. Nevertheless, as we have discussed in Sec. I, there is no reason in the context of QCD why this probability should be zero. In fact, bag models indicate that the mean number of charm quarks in the proton is of order 1%.[5] More generally it may be possible that in lattice calculations or other non-perturbative approaches one may be able to calculate such probabilities (e.g., the mixing of $c\bar{c}$ states in a glueball) because of the heavy quark mass parameters.

We emphasize that although the virtual heavy quark states in a pion or proton are far-off shell, all of the constituents are bound within the hadron because of color forces. This leads inevitably to the pre-

diction that the heavy quarks carry the largest fraction x of the hadronic momentum in the infinite momentum frame for the heavy quark Fock states. This is in striking contrast to the x distribution of heavy quarks created in a high momentum transfer collision by perturbative mechanisms.

The suppression mechanism (described in Sec. IX) for hadronic ψ production at large x_F presumably also has consequences for the decay of the B-meson ($b\bar{q}$) into ψX where the b-quark decays into $c\bar{c}s$. Taking into account all possible decay modes and kinematical suppression one gets in the free quark model $\Gamma(b \to c\bar{c}X)/\Gamma(b \to \text{all}) \sim 14\text{-}20\%$.[38] According to the discussion in Sec. IX we expect a strong suppression ($\sim 10^{-3}$) when instead considering $\Gamma(B \to \psi X)$. Generally speaking, the decay of hadrons into hidden heavy quark states is expected to provide a powerful probe into non-perturbative hadron dynamics.

We have argued on general grounds that the probability of a hadron to contain an intrinsic heavy quark pair should fall as

$$P_{Q\bar{Q}} \propto \frac{\alpha_s^2(Q^2)}{R^2 m_Q^2(Q^2)} \tag{42}$$

where $m_Q(Q^2)$ is the heavy quark running mass at the scale $Q^2 \sim m_Q^2$, and R is a hadron size parameter. If this very slow fall-off in m_Q is correct, there will be copious diffractive large x_L production of heavy quark (b, t) systems in very high energy hadron collisions. Because of the large cross section and the large luminosity possible in hadron-hadron collisions, diffractive production of heavy quarks could become an important method for the discovery and measurement of heavy quark systems.

The presence of intrinsic charm in nucleons makes possible a new array of charged and neutral weak current interactions, the most dramatic one being the charged-current interaction which changes the intrinsic charm quarks into bottom quarks at large x_{Bj}. In particular we predict large neutrino-induced cross sections for b-quark production in the current fragmentation region with $\bar{c}$-quark production in the target fragmentation region.

ACKNOWLEDGMENT

We would like to thank P. Hoyer for contributions in an initial stage of this work and A. Kernan for useful correspondence.

One of us (N. S.) thanks Z. Hioki, J. Leveille, and D. P. Roy for discussions and correspondence. He also wishes to thank the members of the Fermilab Theory Group for their hospitality. This work was supported in part by the Department of Energy under contract DE-AC03-76SF00515 and by the Swedish National Science Research Council under contract F-PD8207-101.

REFERENCES

1. The states are defined at equal $\tau = t + z$ in the light-cone gauge $A^+ = A^0 + A^3 = 0$

2. S. J. Brodsky and G. P. Lepage, Phys. Rev. D22, 2157 (1980) and S. J. Brodsky, Y. Frishman, G. P. Lepage and C. Sachrajda, Phys. Lett. 91B, 239 (1980), and references therein.

3. For example, in Ref. 4 it is shown that the valence $|\bar{u}d\rangle$ Fock state of the pion has a probability $P_V \sim 0.2$ to 0.25, as obtained from the analysis of $\pi^0 \to \gamma\gamma$ and $\pi^+ \to \mu^+\nu$ decays.

4. S. J. Brodsky, T. Huang and G. P. Lepage, SLAC-PUB-2540.

5. J. F. Donoghue, and E. Golowich, Phys. Rev. D15, 3421 (1977).

6. For a review, see S. Wojcicki, SLAC-PUB-2603; A. Kernan, Proc. Photon-Lepton Conf. at Fermilab, 1979, p. 535.

7. K. L. Giboni et al., Phys. Lett. 85B, 437 (1979) and A. Kernan, private communication.

8. D. Drijard et al., Phys. Lett. 81B, 250 (1979); W. Geist, Proc. of the Topical Workshop on Forward Production of High-Mass Flavors at Collider Energies, College de France, Paris, 1979; G. Sajot, Proc. XXth Int. Conf. on High Energy Physics, Madison, Wisconsin, 1980.

9. W. Lockman et al., Phys. Lett. 85B, 443 (1979).

10. D. Drijard et al., Phys. Lett. 85B, 452 (1979).

11. A. Chilingarov et al., Phys. Lett. 83B, 136 (1979).

12. L. J. Koester et al., paper submitted to the XXth Int. Conf. on High Energy Physics, Madison, Wisconsin, 1980.

13. Diffractive production of charm was suggested by G. Gustafson and C. Peterson, Phys. Lett. 67B, 81 (1977).

14. E. Golowich, Phys. Rev. 18, 927 (1978); S. J. Brodsky and J. F. Gunion, Phys. Rev. 19, 1005 (1979). Some of these higher particle Fock states can also be associated in part with the meson cloud around the nucleon and peripheral or Deck diagrams involved in low momentum transfer reactions.

15. For a review, see C. Peterson, Proc. of the Topical Workshop on Forward Production of High-Mass Flavors at Collider Energies, College de France, Paris, 1979.

16. S. J. Brodsky, P. Hoyer, C. Peterson and N. Sakai, Phys. Lett. 93B, 451 (1980).

17. S. J. Brodsky and C. Peterson, in preparation.

18. M. Suzuki, Phys. Lett. 71B, 139 (1977); J. D. Bjorken, Phys. Rev. D17, 171 (1978).

19. A. J. Buras and K.J.F. Gaemers, Nucl. Phys. B132, 249 (1978).

20. A. R. Clark et al., LBL-10879.

21. J. P. Leveille and T. Weiler, Nucl. Phys. B147, 147 (1979).

22. See, e.g. H. M. Georgi et al., Ann. Phys. (N.Y.) 114, 273 (1978).

23. M. G. Albrow et al., Nucl. Phys. B108, 1 (1976).

24. H. Wachsmuth, Proc. of the Lepton-Photon Conf. at Fermilab, 1979.

25. For a review, see L. L. Chan Wang, BNL-27615-R.

26. We have ignored the threshold suppression originating from a slow rescaling variable; see, e.g. R. M. Barnett, Phys. Rev. Lett. 36, 1163 (1976).

27. M. Holder et al., Phys. Lett. 69B, 377 (1977); R. Brandelik et al., Phys. Lett. 70B, 387 (1977).

28. M. Holder et al., Phys. Lett. 70B, 396 (1977); A. Benvenuti et al., Phys. Rev. Lett. 41, 725 (1978); J.G.H. de Groot et al., Phys. Lett. 86B, 103 (1979); T. Trinko et al., Univ. of Wisconsin preprint.

29. H. Goldberg, Phys. Rev. Lett. 39, 1598 (1977).

30. N. Armenise et al., Phys. Lett. 94B, 527 (1980).

31. M. Holder et al., Phys. Lett. 74B, 277 (1978).

32. L. M. Sehgal, Nucl. Phys. B65, 141 (1973).

33. J. E. Kim et al., Univ. of Pennsylvania preprint UPR-158T.

34. H. Wachsmuth, preprint CERN/EP/Phys.77-43.

35. The same conclusion has been reached independently by R. Phillips, Rutherford preprint RL-80-061.

36. J. Badier et al., Proc. Lepton-Photon Conf. at Fermilab, 1979, p. 161; CERN/EP 79-61.

37. Another alternative way of understanding this suppression is to take into account the mismatch of the wave function of ψ and the intrinsic charm state, because the intrinsic charm state has presumably a smaller transverse momentum spread compared to ψ.

38. H. Fritzsch, Phys. Lett. 86B, 343 (1979).

39. M. Kobayashi and T. Maskawa, Prog. Theor. Phys. 49, 652 (1973).

40. See, e.g., M. B. Einhorn and S. D. Ellis, Phys. Rev. D12, 2007 (1975); C. E. Carlson and R. Suaya, Phys. Rev. D18, 760 (1978).

FIGURE CAPTIONS

Fig. 1. Diagrams which give rise to the intrinsic heavy quarks ($Q\bar{Q}$) within the proton. Curly and dashed lines represent transverse and logitudinal-scalar (instantaneous) gluons, respectively.

Fig. 2. Same sign dimuon pair production from the intrinsic charm component of nucleons.

Fig. 3. $d\sigma/d|x|$ for Λ^o at 53 GeV and Λ_c^+ at 53 and 63 GeV.[7,8,9] The smooth curve is a fit to the Λ^o data points.

Fig. 4. $d\sigma/dx$ for[10] D^+ and[11] D^o at $\sqrt{s}$ = 53 GeV.

Fig. 5. x_F - distribution of events in D - peak found in π-p interactions at $\sqrt{s}$ = 20 GeV.[13]

Fig. 6. Diffractive production of open charm from the intrinsic charm component of nucleons.

Fig. 7. a) Example with contribution to the deep inelastic structure functions from an extrinsic quark q; b) from an intrinsic quark q.

Fig. 8. The x distribution of the charmed quark in a D-meson.

Fig. 9. The x distribution of the charmed quark in a $|uudc\bar{c}\rangle$ state.

Fig. 10. The x distribution of a light quark in a $|uudc\bar{c}\rangle$ state.

Fig. 11. Comparison of the x-distribution of the charm quark in the intrinsic sea (solid line) and the sea calculated from perturbative QCD[19] at Q^2 = 50 GeV^2 (dashed line).

Fig. 12. Lepto-production of charm from the intrinsic charm sea and via the photon-gluon fusion model, respectively.

Fig. 13. The x distribution of the charm quark in the $|u\bar{d}c\bar{c}\rangle$ state.

Fig. 14. The x distribution of the light quark in the $|u\bar{d}c\bar{c}\rangle$ state.

Fig. 15. The x distribution of the Λ_c from the intrinsic charm component of the proton.

Fig. 16. The x distribution of the D^- from the intrinsic charm component of the proton.

Fig. 17. The x distribution of the D meson from the intrinsic charm component of the pion.

Fig. 18. a) Production of b-quark from the intrinsic charm component of the proton; b) Decay of b-quark into μ^+.

Fig. 19. Energy dependence of the production cross section of b quarks (solid and dashed lines corresponding to two V_{cb} - solutions) and t-quarks (dotted line).

Fig. 20. The ratio of the same sign dimuon events to the normal charged current events. The solid and dashed-dotted lines are theoretical prediction from the intrinsic charm component for $\mu^+\mu^+$ and $\mu^-\mu^-$, respectively using $V_{cb} = 0.48$. Data from Ref. 28. Also shown (dotted line) is the QCD first-order prediction.[29]

Fig. 21. Production of t-quark from the intrinsic b component of hadron.

Fig. 22. Exclusive production of strange/charm baryons and charm/beauty baryons.

Fig. 23. Wrong sign single muon production from the intrinsic charm component.

Fig. 24. The $c\bar{c}$ mass spectrum in the intrinsic charm state $|uudc\bar{c}\rangle$. The shaded area corresponds to the χ, η_c, ψ and ψ' production.

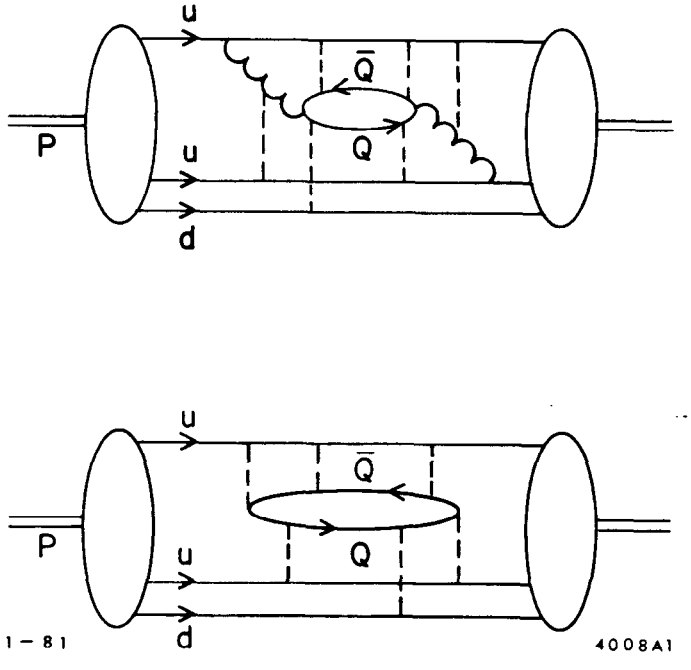

Fig. 1

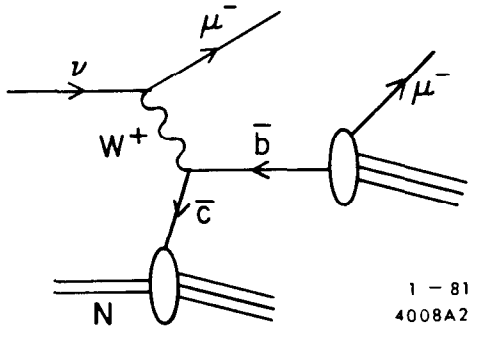

Fig. 2

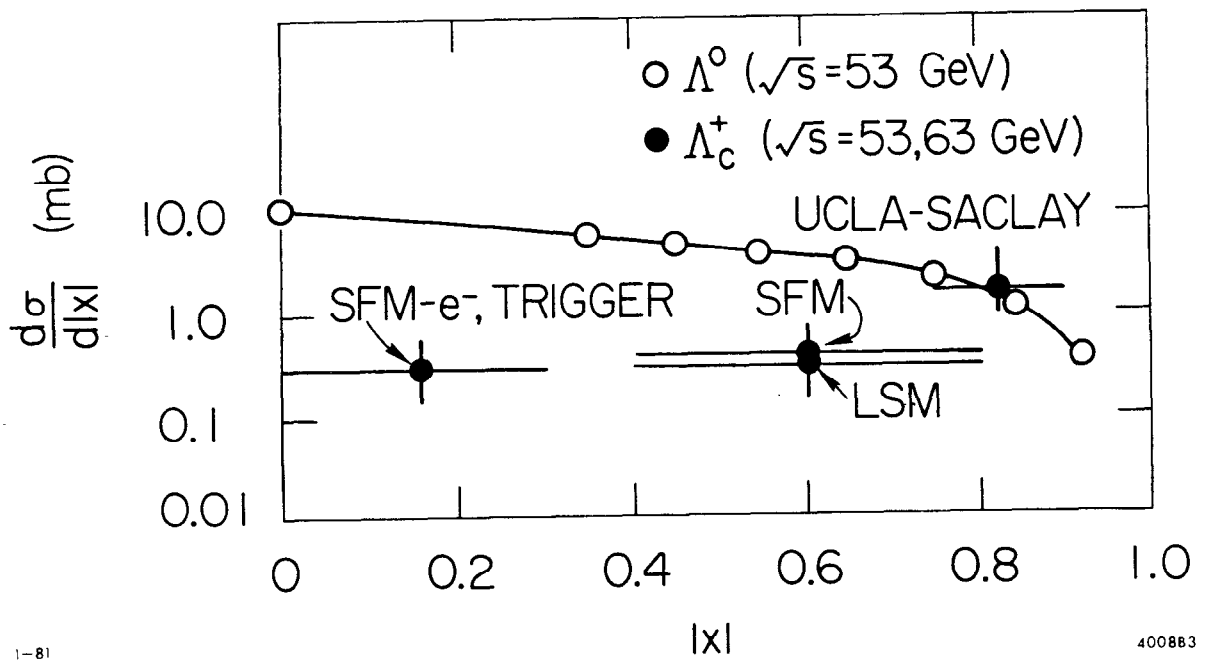
o Λ° (√s=53 GeV)
● Λc+ (√s=53,63 GeV)
UCLA-SACLAY
SFM-e⁻, TRIGGER
SFM
LSM
dσ/d|x| (mb)
10.0
1.0
0.1
0.01
0
0.2
0.4
0.6
0.8
1.0
|x|
1-81
400883

Fig. 3

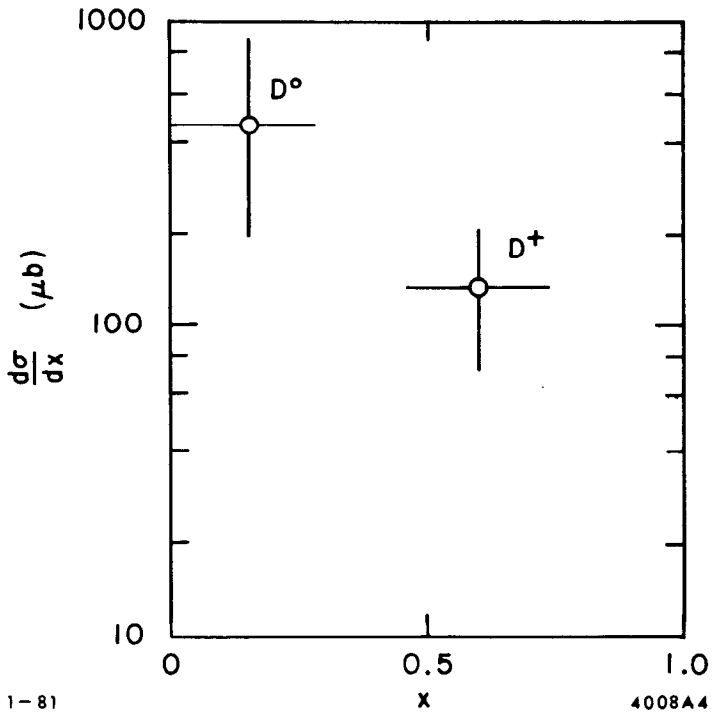

Fig. 4

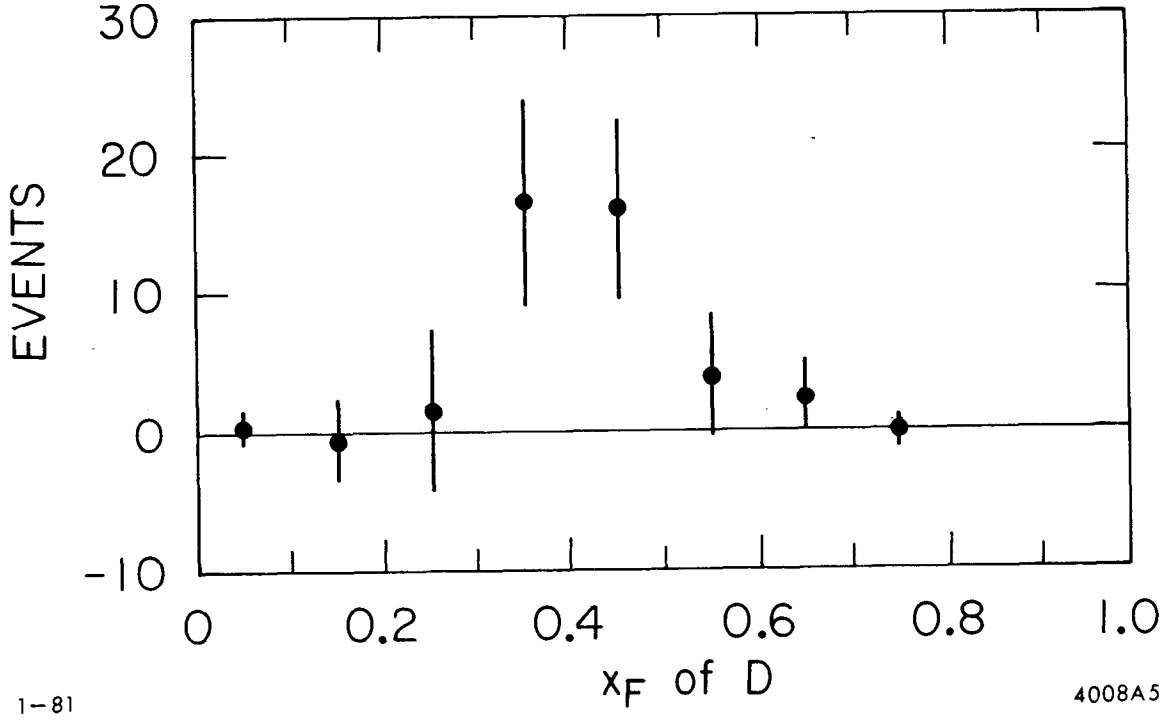

Fig. 5

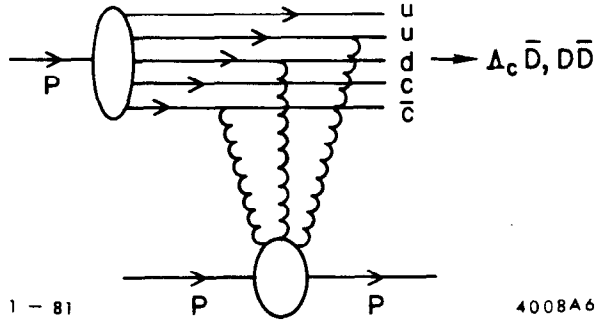

Fig. 6

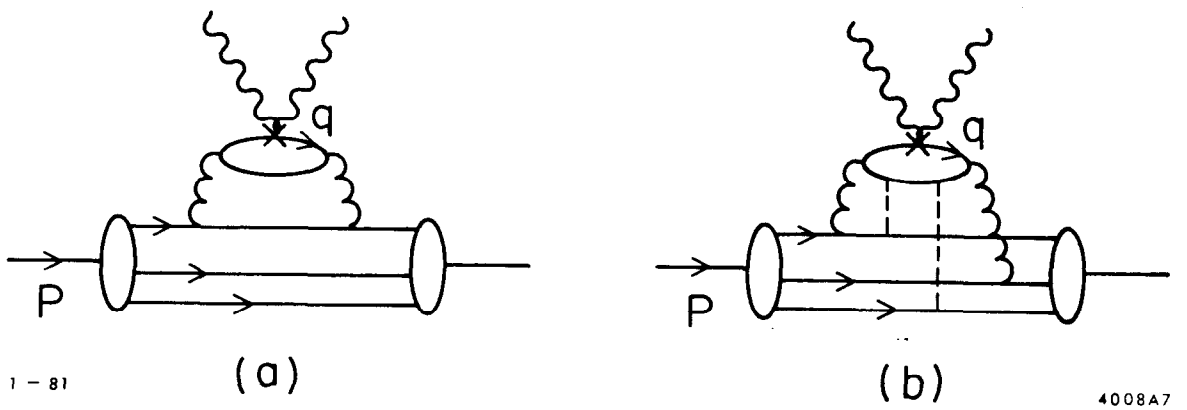

Fig. 7

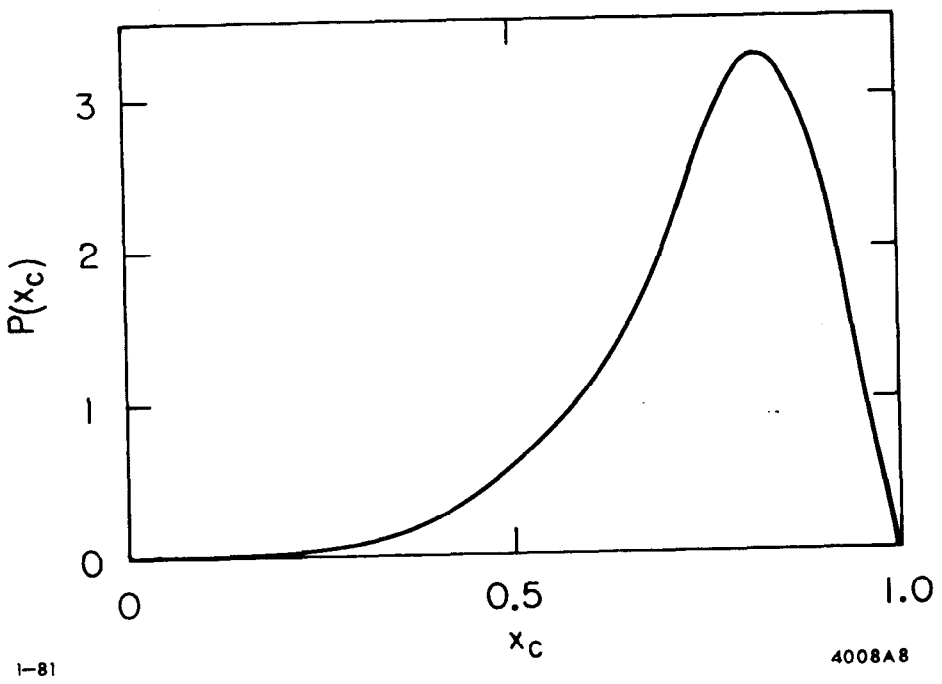

Fig. 8

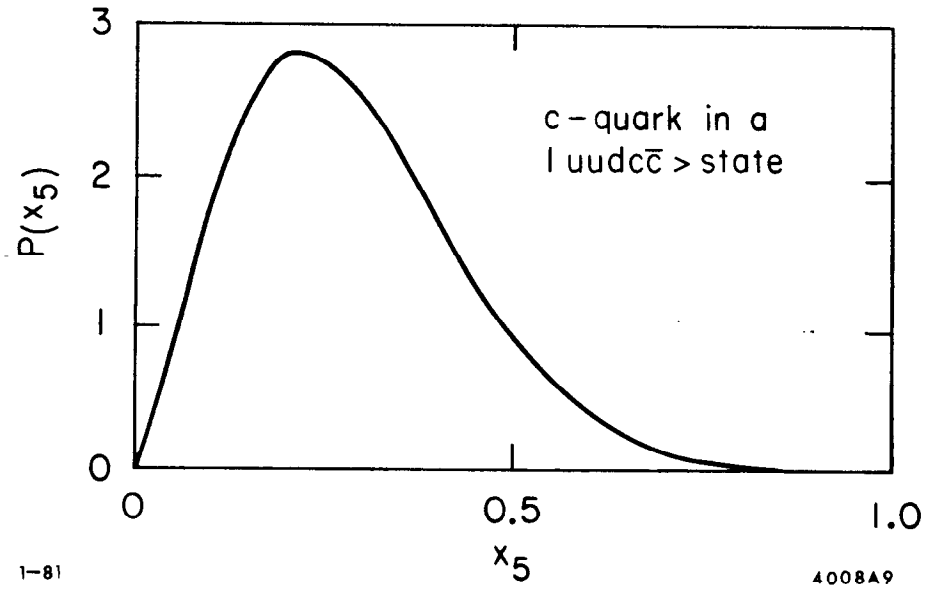

Fig. 9

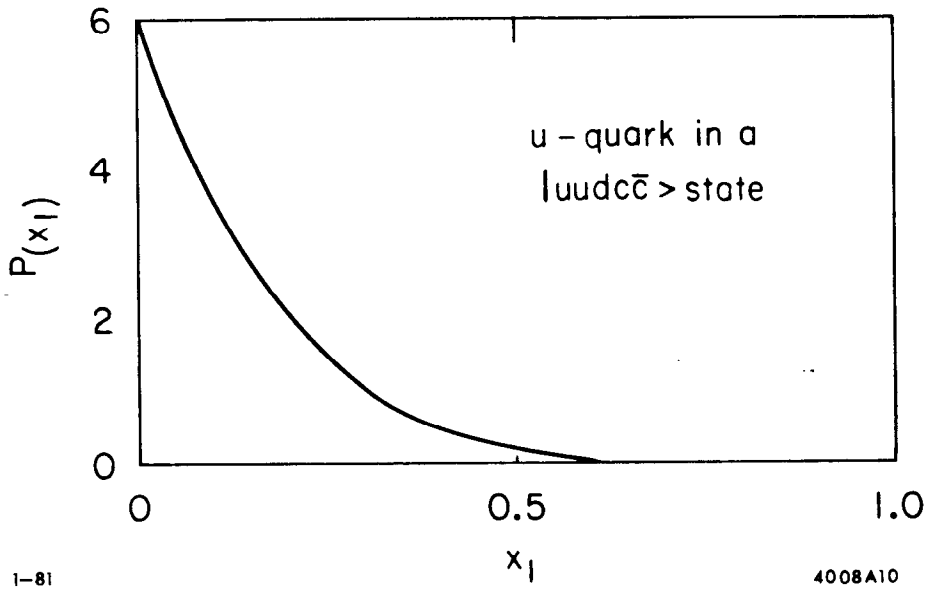

Fig. 10

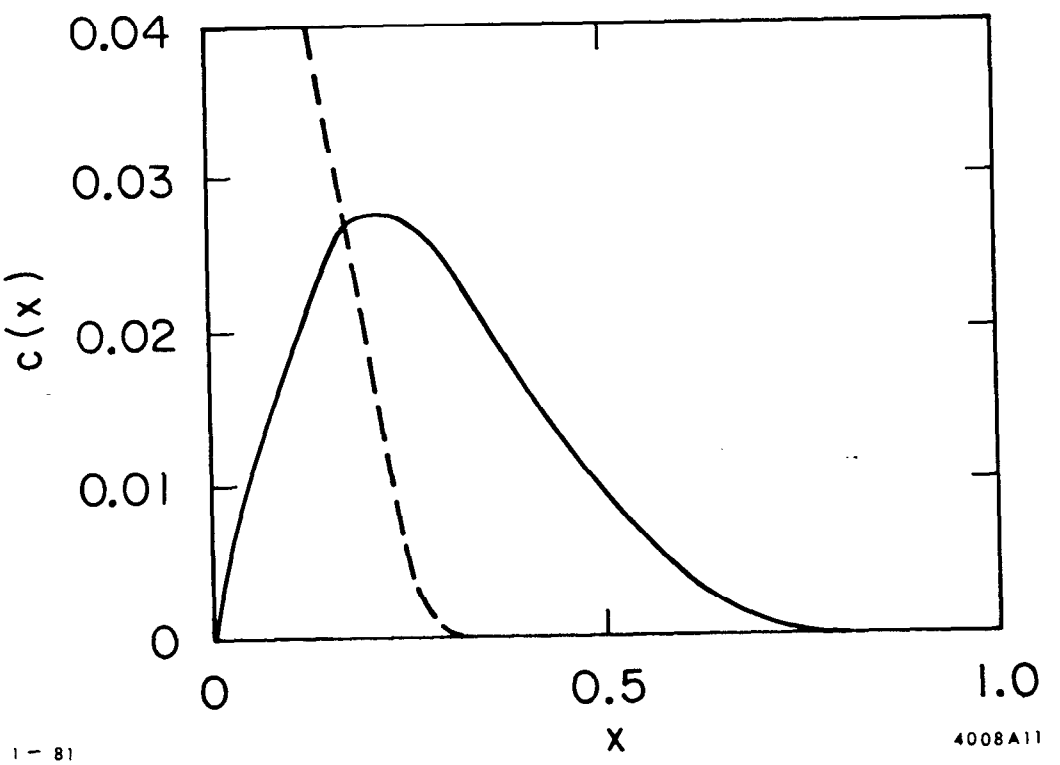

Fig. 11

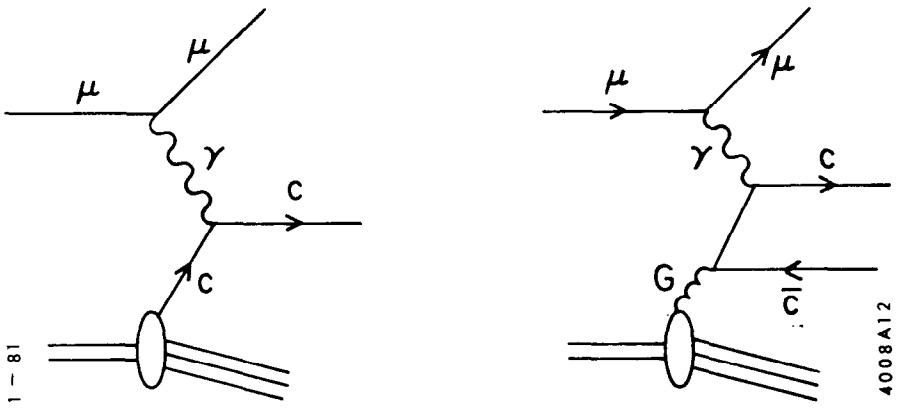

Fig. 12

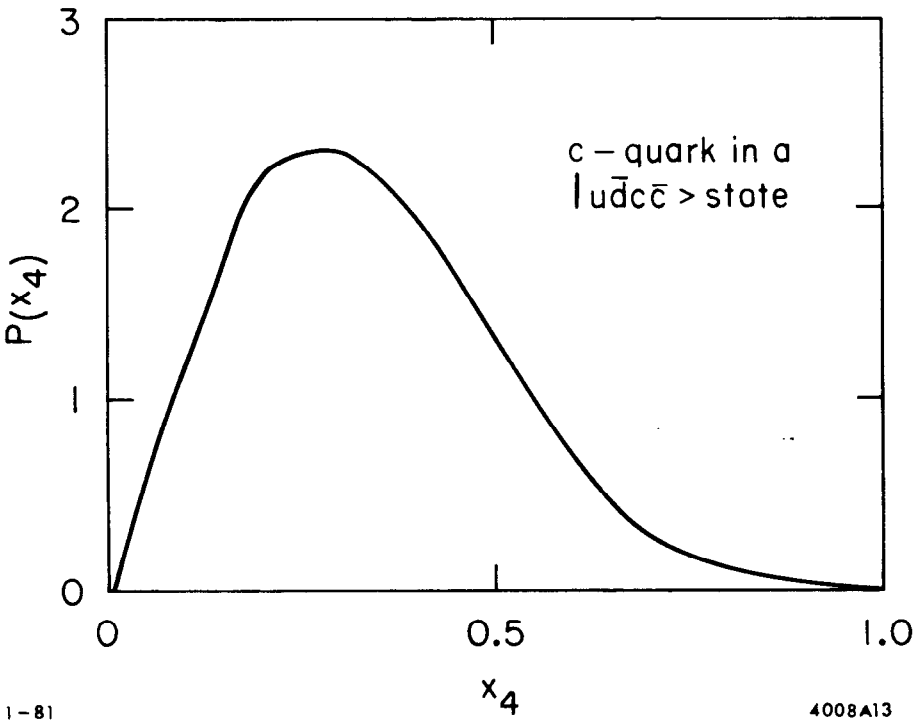

Fig. 13

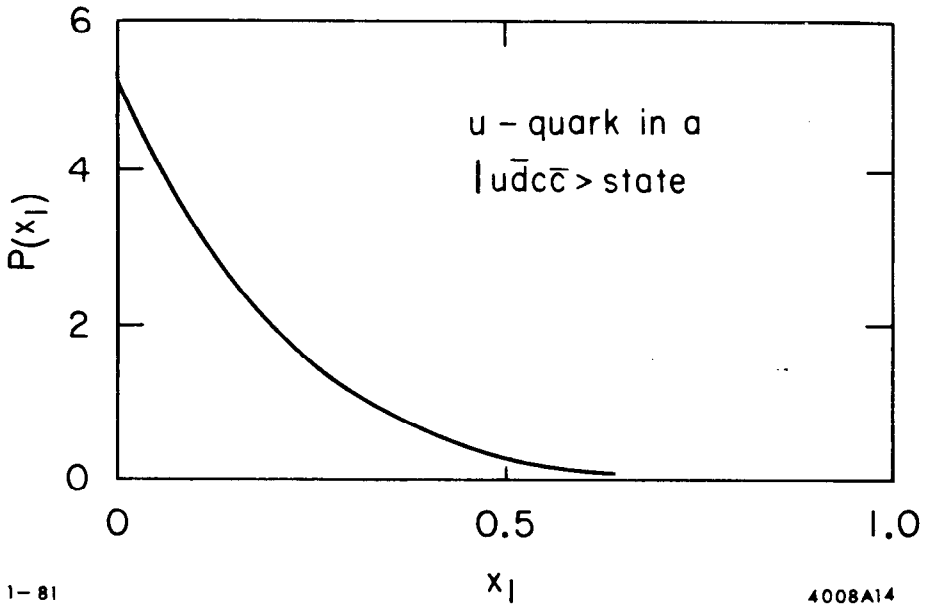

Fig. 14

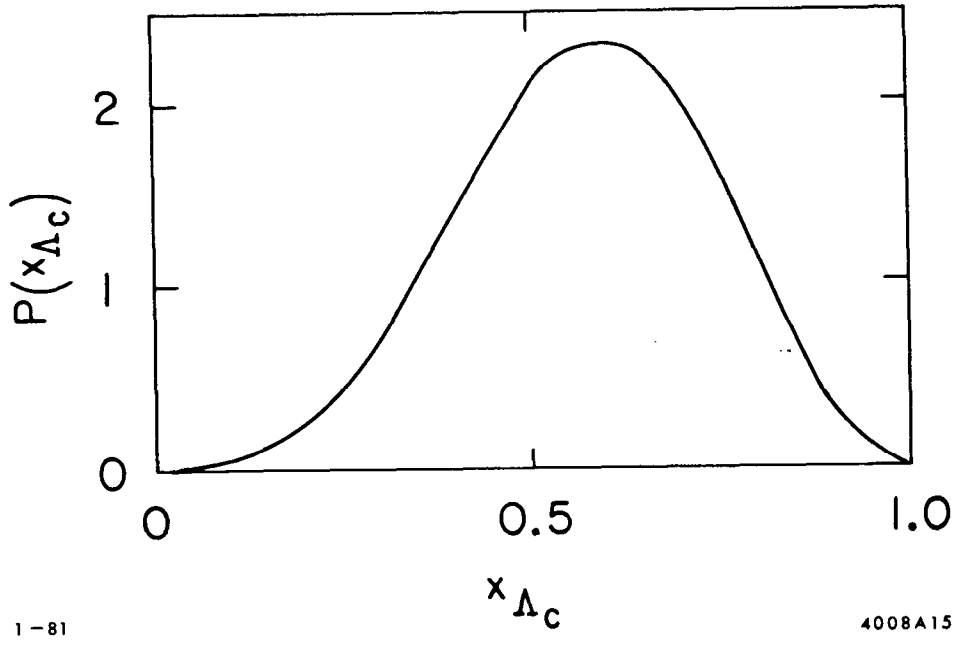

Fig. 15

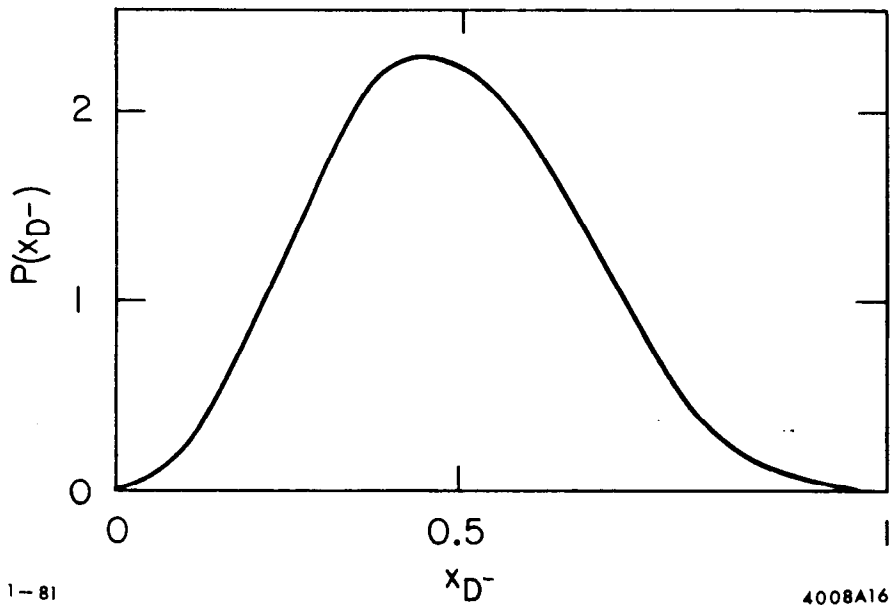

Fig. 16

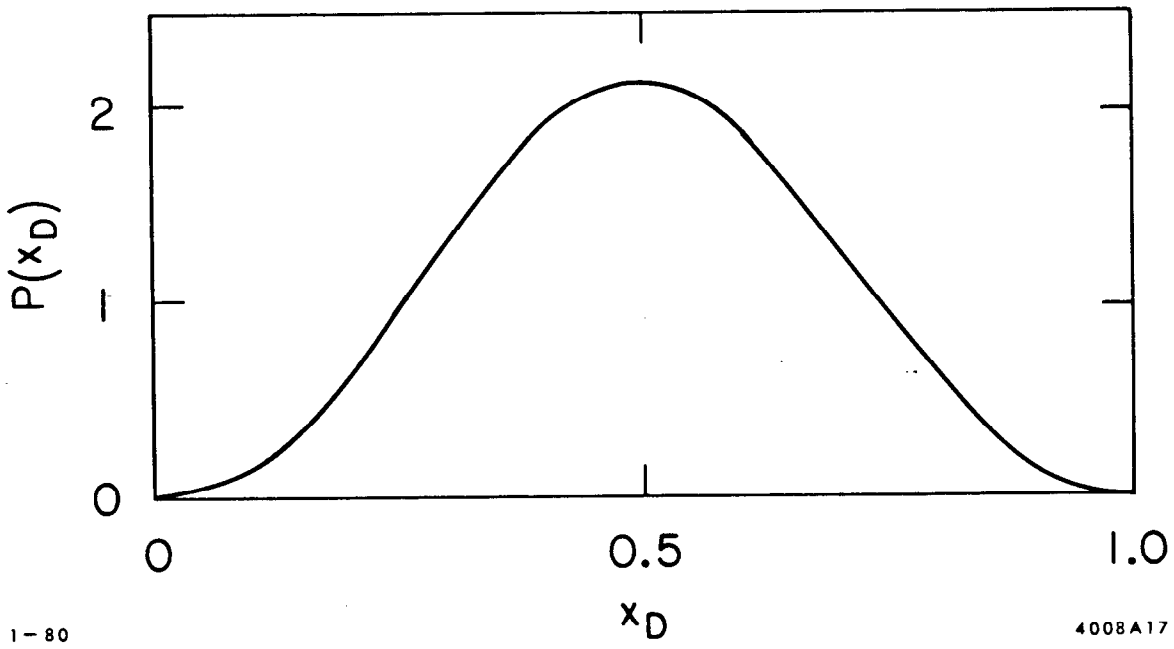

Fig. 17

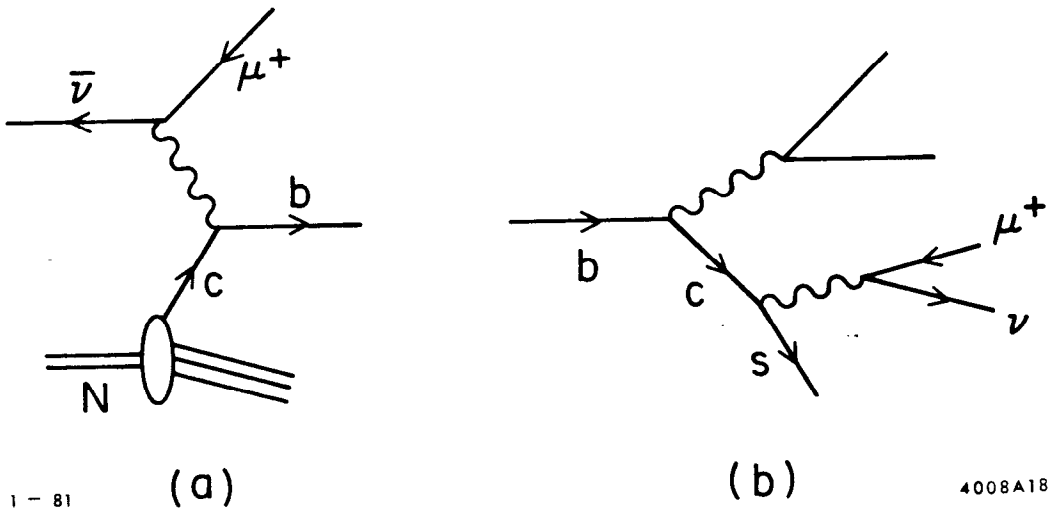

Fig. 18

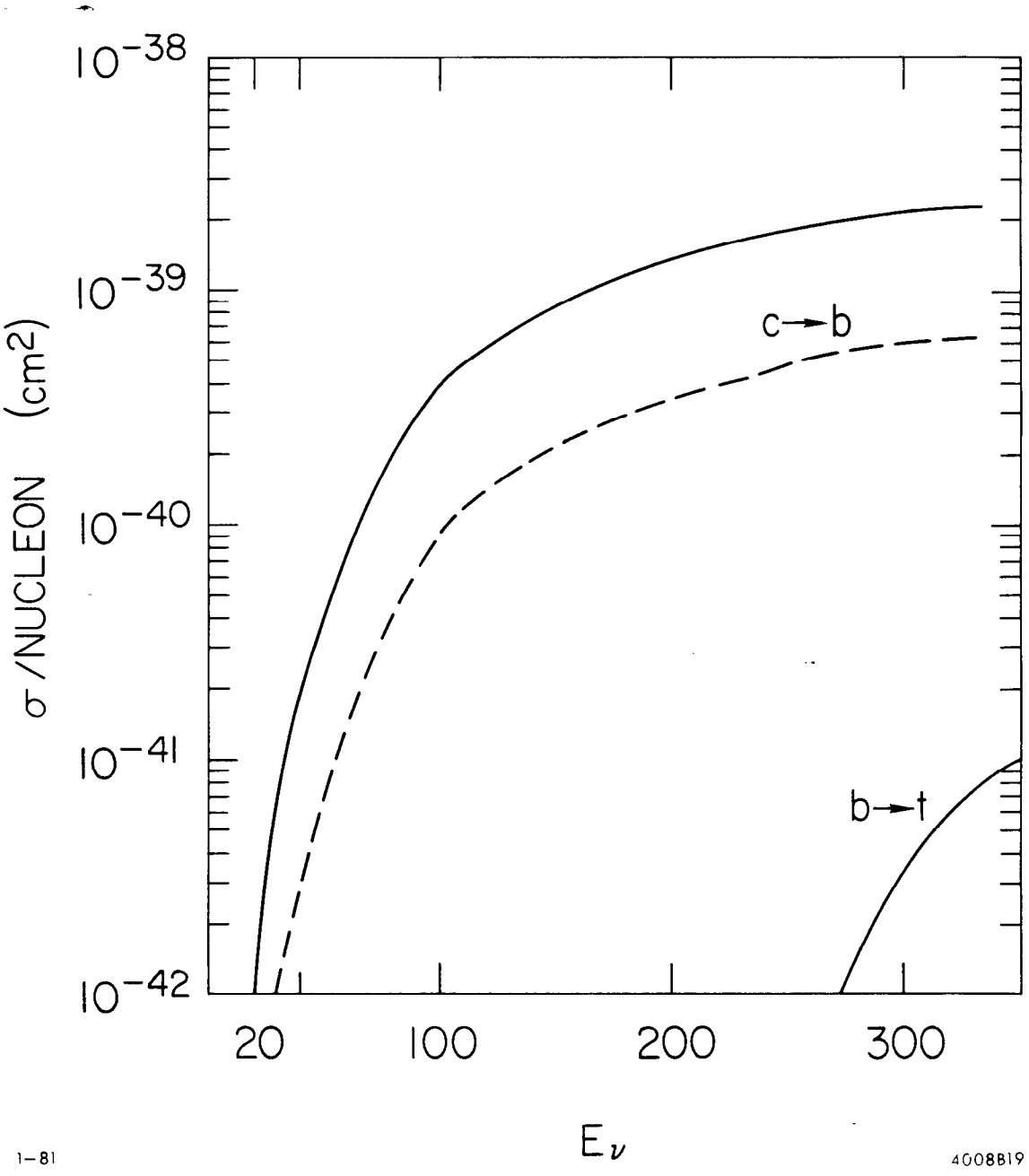
10^{-38}
10^{-39}
10^{-40}
10^{-41}
10^{-42}
σ/NUCLEON (cm²)
c→b
b→t
20
100
200
300
E_ν
1-81
4008B19

Fig. 19

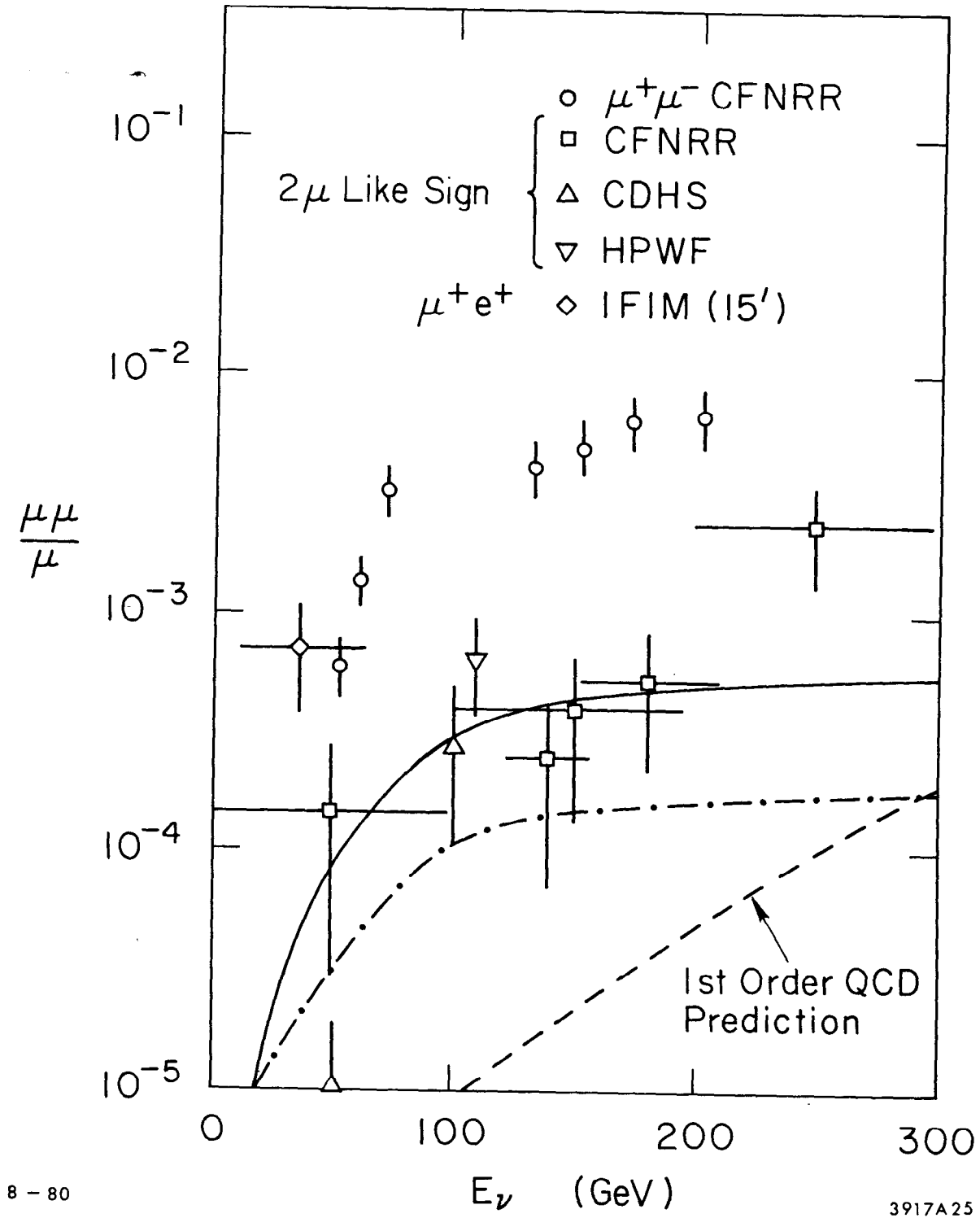
$\mu^+\mu^-$ CFNRR
CFNRR
2μ Like Sign
CDHS
HPWF
μ^+e^+
IFIM (15′)
10^{-1}
10^{-2}
10^{-3}
10^{-4}
10^{-5}
$\frac{\mu\mu}{\mu}$
1st Order QCD Prediction
0
100
200
300
E_ν (GeV)
8 – 80
3917A25

Fig. 20

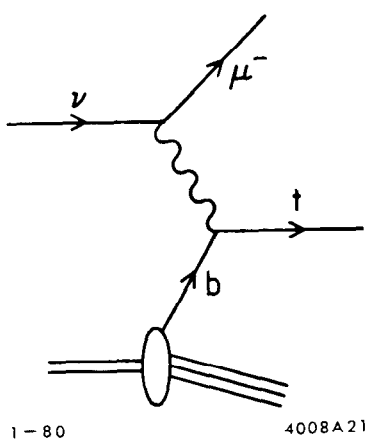

Fig. 21

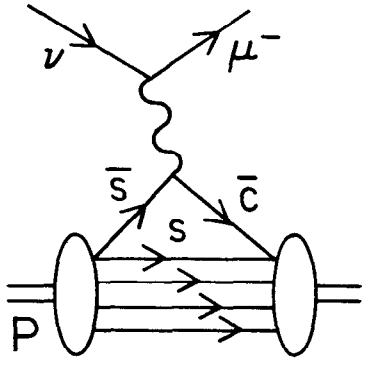

1–81 (a)

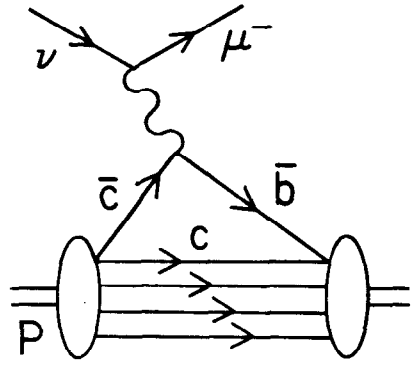

(b) 4008A22

Fig. 22

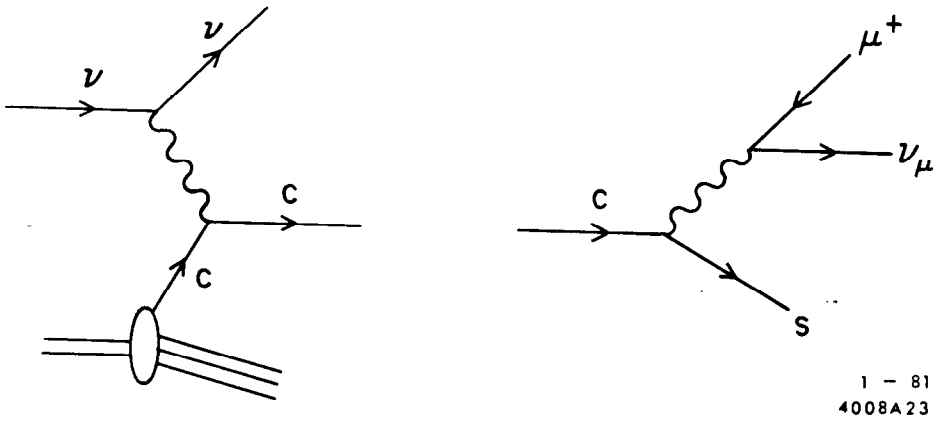

Fig. 23

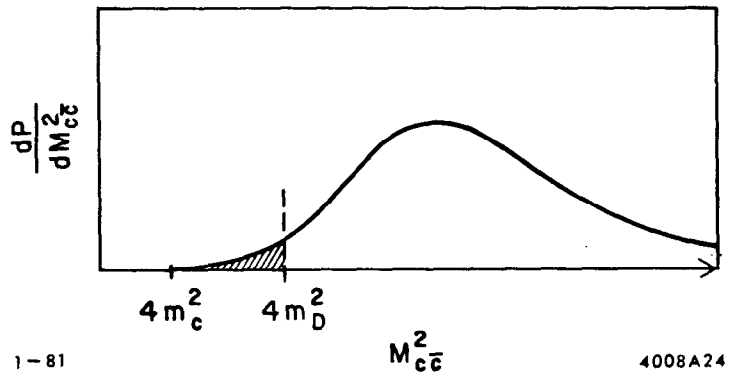

Fig. 24